RECENT RESULTS FROM THE KAMLAND-ZEN EXPERIMENT

T. O'DONNELL
for the KamLAND-Zen Collaboration
Department of Physics, University of California Berkeley, and
Nuclear Science Division, Lawrence Berkeley National Laboratory, Berkeley, CA 94720, USA

The KamLAND-Zen experiment is a new application of the KamLAND detector running in parallel with the ongoing antineutrino program at KamLAND. The experiment searches for neutrinoless double beta decay of ^{136}Xe using a target of Xe-loaded liquid scintillator placed at the center of the KamLAND detector. KamLAND-Zen has completed its first phase of running, corresponding to the largest exposure of ^{136}Xe to date: 89.5 kg-yr. Based on the first-phase dataset the collaboration obtains a lower limit for the neutrinoless double-beta decay half-life of ^{136}Xe: $T^{0\nu}_{1/2} > 1.9 \times 10^{25}$ yr at 90% C.L. Combining limits from KamLAND-Zen and EXO-200 gives $T^{0\nu}_{1/2} > 3.4 \times 10^{25}$ yr at 90% C.L. In this talk we present the results of the first-phase data set and the implications for the neutrinoless double beta decay detection claim in ^{76}Ge reported by a part of the Heidelberg-Moscow collaboration.

1 Double Beta ($\beta\beta$) Decay

1.1 Two neutrino double beta decay ($2\nu\beta\beta$)

This is the simultaneous decay of two neutrons in a nucleus, emitting two electrons and two antineutrinos. The process is allowed in the Standard Model but is second order in the weak interaction and is thus extremely rare. Despite this rarity, $2\nu\beta\beta$ decay has been observed in about a dozen different nuclei; the measured halflives range between $10^{19} \sim 10^{21}$ years[?].

1.2 Neutrinoless double beta decay ($0\nu\beta\beta$)

This is a hypothetical $\beta\beta$ decay mode in which two neutrons decay, emitting two electrons and no neutrinos. The occurance of such decays would imply neutrinos are Majorana particles. The halflife for $0\nu\beta\beta$ decay ($T^{0\nu}_{1/2}$) mediated by the exchange of a light virtual Majorana neutrino is: $(T^{0\nu}_{1/2})^{-1} = G^{0\nu}|M^{0\nu}|^2 m^2_{\beta\beta}$, where $G^{0\nu}$ is the phase space factor for the decay, $|M^{0\nu}|$ is the nuclear matrix element (NME) connecting the initial and final nuclei, and $m_{\beta\beta}$ is called the effective Majorana neutrino mass. This last parameter is connected to the absolute neutrino masses in the following way: $m_{\beta\beta} = |\sum_{i=1}^{3} U^2_{ei} m_i|$. Here the U_{ei} are elements of the Pontecorvo-Maki-Nakagawa-Sakata (PMNS) mixing matrix and the m_i are the masses of the neutrino mass states.

While the mixing angles in the standard PMNS matrix are well constrained experimentally, there are to date no direct measurements of the m_i. The possibility to probe the Dirac-or-Majorana nature of the neutrino and the potential to constrain the m_i directly are among the motivations for $\beta\beta$ decay searches [?].

1.3 Experimental searches for neutrinoless double beta decay

$\beta\beta$ decay searches generally proceed by measuring the summed energy spectrum of the final state electrons and looking for evidence of zero-neutrino emission. For $0\nu\beta\beta$ decay via the mechanism described above, the signature in an ideal detector would be particularly prominent — since the electrons carry off all the decay energy [a] a peak in the spectrum at the Q-value of the transition would be observed. The intensity of the peak can be related to $T^{0\nu}_{1/2}$ and ultimately $m_{\beta\beta}$.

Interpreting results of $0\nu\beta\beta$ searches in terms of $m_{\beta\beta}$ is challenged by significant theoretical uncertainty on NME predictions — estimates typically vary by a factor of ~ 2 depending on the calculation method used [?]. To get a sense of the experimental challenge involved we note that if $0\nu\beta\beta$ decay proceeds via the mechanism mentioned above, with $m_{\beta\beta} = 50$meV, then the expected halflives range between $10^{25} \sim 10^{27}$ years depending on the nuclear system and the NME used.

There is a claim for detection of $0\nu\beta\beta$ decay of ^{76}Ge [?], however this claim is controversial and is generally not accepted as a compelling observation. The sensitivity necessary to test this claim is a common benchmark $0\nu\beta\beta$ experiments. We note, however, that direct comparison of $m_{\beta\beta}$ limits from different nuclei is complicated by the NME uncertainty.

2 KamLAND-Zen

The KamLAND-Zen experiment, focussing on ^{136}Xe, is one of several ongoing $0\nu\beta\beta$ searches. The experiment is hosted inside the existing KamLAND detector and began taking data in September 2011 [?]. The KamLAND detector is housed in an 18-m-diameter, spherical stainless-steel tank (SST), the inner surface of which is instrumented with 1879 large-area photocathode photomultiplier tubes (PMTs) providing $\sim$ 34% photocathode coverage. The SST contains $\sim$ 1 kton of ultrapure liquid scintillator (LS) which is constrained by a thin (135μm thick) transparent balloon to an approximately spherical volume of radius 6.5 m. The center of the LS volume coincides with the center of the SST. The LS-filled balloon, supported by thin ropes, is suspended in a volume of transparent non-scintillating mineral oil which fills the region between the outer surface of the balloon and the inner surface of the SST. Outside the SST is a 3.2 kton water Cherenkov detector which provides a cosmic ray muon veto.

KamLAND-Zen consists of an inner balloon (diameter 3.08 m) which is suspended at the center of the KamLAND LS. This balloon is made from 25μm thick, transparent nylon film and is filled with approximately 13 tons of Xe-load LS. The Xe-loading fraction is $\sim$2.5% by weight, and is enriched to 90.93 ± 0.05% in ^{136}Xe. This amounts to a total ^{136}Xe mass of $\sim 300\,kg$.

Scintillation light is detected by the PMT array, the position and energy of decays in the LS are reconstructed from the PMT hit-time and hit-charge distributions. The position resolution is $\sigma_R \sim 15\,cm/\sqrt{E(\mathrm{MeV})}$ and the energy resolution is $\sigma_E/E = (6.6\pm0.3)\%/\sqrt{E(\mathrm{MeV})}$. Ultimately the data analysis is carried out in terms of reconstructed energy which we denote E_{vis}. A detector response model is used to construct the expected E_{vis} spectrum of decays in the LS. The model accounts for the energy resolution and particle- and energy-dependant non-linearities such as scintillator quenching and energy loss due to Cherenkov emission. The unsmeared visible energy is assumed to be related to the real energy deposited by a particle in the LS in the following way:

$$\Delta E_{vis} = A \cdot \left\{ \frac{1}{1+R} \cdot \frac{1}{1 + k_B \cdot dE/dx} + \frac{R}{1+R} \cdot \frac{dN_{Ch}}{dE} \right\} \Delta E \,. \quad (1)$$

[a] We neglect here the recoil energy of the nucleus

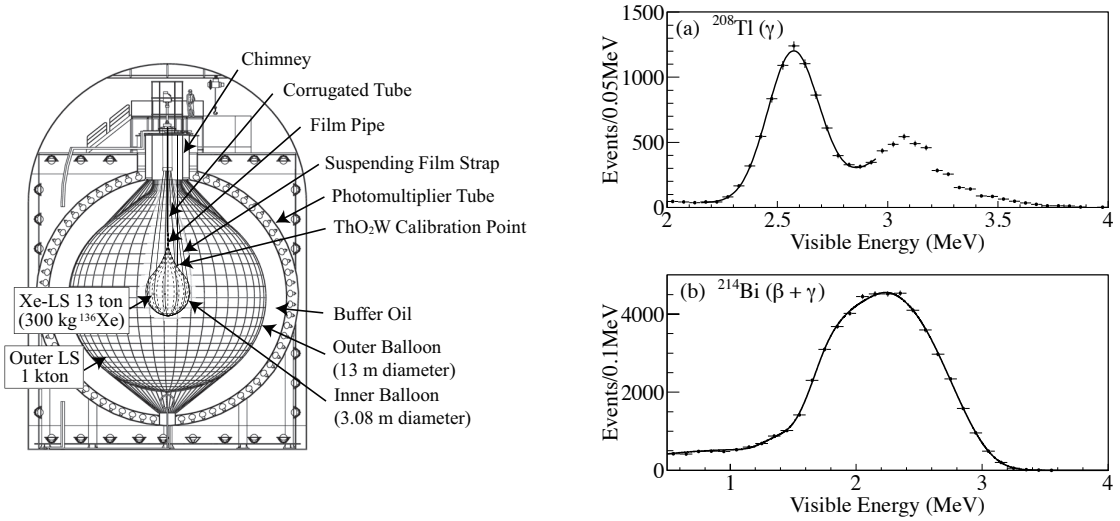

Figure 1: (Left) Schematic of the KamLAND/KamLAND-Zen detector. (Right Top) Visible energy spectrum of ^{208}Tl events from calibration source deployment together with the best fit model. (Right Bottom) Visible energy spectrum of tagged ^{214}Bi $(\beta + \gamma)$ events in the Xe-LS together with the best fit model.

Here A is a normalization factor, the value is chosen so that the visible energy of gammas from neutron capture on protons coincides with their real energy (2.22 MeV); dE/dx is the stopping power of the particle; k_B, known as Birk's constant, is an empirical constant that must be determined for the scintillator; dN_{Ch}/dE is the Cherenkov photon yield per unit energy and R parametrizes the relative contribution of scintillation and Cherenkov photons to the photo-electron yield in the PMT array. The final visible energy distribution is obtained by applying a gaussian energy resolution with a width $\sigma_E/E = (6.6 \pm 0.3)\%/\sqrt{E(\mathrm{MeV})}$.

The parameters of the detector response model, A, k_B, R and σ_E are determined using (i) calibration data from a ^{208}Tl γ-ray source positioned in the KamLAND-LS at the edge of the Xe-LS volume and (ii) tagged $\beta+\gamma$ events in the Xe-LS from ^{214}Bi — these events are tagged by their time and spatial correlation with ^{214}Po. The visible energy distributions of ^{208}Tl calibration data and the tagged ^{214}Bi sample together with the best-fit model are shown in right panel of Figure **??**. The stability of the detector response is monitored using spallation neutron capture gammas and is found to be stable to within 1%.

2.1 First phase dataset

The first phase of data set ran from October 12 2011 to June 14 2012. The dataset is divided into two parts, denoted DS1 and DS2. DS1 ran until Feb 2012 at which point some plumbing hardware — a long teflon pipe with a stainless steel inlet — was introduced into the Xe-LS volume to facilite a LS-filtration campaign undertaken to reduce backgrounds. This hardware remained in place after the filtration campaign ended. The second period, DS2, refers to data taken with this condition. Table **??** summarises the dataset and exposure.

2.2 Event selection

The cuts applied to select candidate events for the $\beta\beta$ analysis are listed below.

(i) Candidates are required to have $0.5 < E_{\mathrm{vis}}(\mathrm{MeV}) < 4.8$, this excludes low energy events where backgrounds are relatively high; 82% of the expected E_{vis} spectrum of $2\nu\beta\beta$ decays falls within this window.

(ii) Fiducial volume (FV) cuts are imposed to reduce backgrounds from detector materials. For DS1 candidates are required to reconstruct within 1.35 m of the detector center, in DS2

candidates are further required to reconstruct outside a 0.2-m-radius cyclinder centered on the teflon pipe and outside a 1.2-m-radius sphere centered on the stainless steel inlet.

(iii) Events occuring within $2\,ms$ after muons are rejected, this removes spallation neutron backgrounds.

(iv) Events occurring within $3\,ms$ of each other are removed, this takes advantage of ^{214}Bi-^{214}Po coincidence decays to exclude background from ^{214}Bi. Inverse beta decays induced by reactor antineutrinos are also rejected because of the delayed coincidence of positrons and neutrons.

(v) A reconstruction quality cut is imposed to remove poorly reconstructed events, from calibration data we estimate this cut reduces the selection efficiency by $< 0.1\%$.

The FV cuts reduce the ^{136}Xe target mass to 179 kg and 125 kg for DS1 and DS2 respectively. The selection efficiency for candidates inside the FV and energy window is 99.8% and 97.9% respectively for $0\nu\beta\beta$ and $2\nu\beta\beta$ events.

2.3 Backgrounds

Some classes of background remain after the candidate selection cuts. We divide these into three catagories described below.

1. Xe-LS backgrounds: These come from residual radioactivity in the Xe-LS, mainly ^{85}Kr, ^{210}Bi and trace amounts of ^{238}U, ^{232}Th and their daughters. The ^{222}Rn-^{210}Pb subchain of ^{238}U and the ^{228}Th-^{208}Pb subchain of the ^{232}Th series are constrained respectively by ^{214}Bi-^{214}Po and ^{212}Bi-^{212}Po sequential decay studies. Other daughters are unconstrained because of a possible break from equilibrium. We also consider the possibility that trace amounts of longlived fallout isotopes, for example ^{134}Cs, ^{88}Y, ^{110m}Ag, may have been introduced into the Xe-LS following the Fukushima Nuclear accident in March 2011.
2. Spallation backgrounds: The largest spallation backgrounds are expected from ^{11}C and ^{10}C which are continuously produced by muon spallation of ^{12}C. Their production rates have been previously measured at KamLAND [?]. There is not much data on spallation products of Xe, but backgrounds from short-lived [b] products are constrained to be negligible from a study of muon time-correlated events in KamLAND-Zen.
3. Backgrounds from the IB and filtration hardware: These come from decays in and on the IB and filtration hardware that reconstruct inside the FV due to the vertex resolution. A study of events reconstructing near the IB is used to measure the IB activity. Decays of ^{214}Bi are evident, there is also evidence for activity from ^{134}Cs,^{137}Cs and ^{110m}Ag contamination which was likely introduced following the Fukushima accident. A Monte Carlo simulation is used estimate the residual activity reconstructing inside the FV.

2.4 Fit to candiate spectrum

The left panel of Figure **??** shows the E_{vis} spectrum of selected candidates as well as the best-fit spectral decomposition from a binned likelihood fit. A peak is apparent at $\sim$ 2.6 MeV, above the ^{136}Xe Q-value (2.458 MeV). We conclude from a spectral and time analysis that this peak is likely due to ^{110m}Ag contamination [?]. The parameters of the model used to fit candidate spectrum are summarized on Table **??**. For the signal and background components, the parameters refer to the normalization of the component in the model, the E_{vis} spectrum of each component is found by applying the detector response model to the expected real energy spectrum. For parameters indicated as constrained, the parameter is allow to vary in the fit but is constrained by a likelihood penalty term to the range of values allowed by some other

[b] lifetimes of less than 100 s

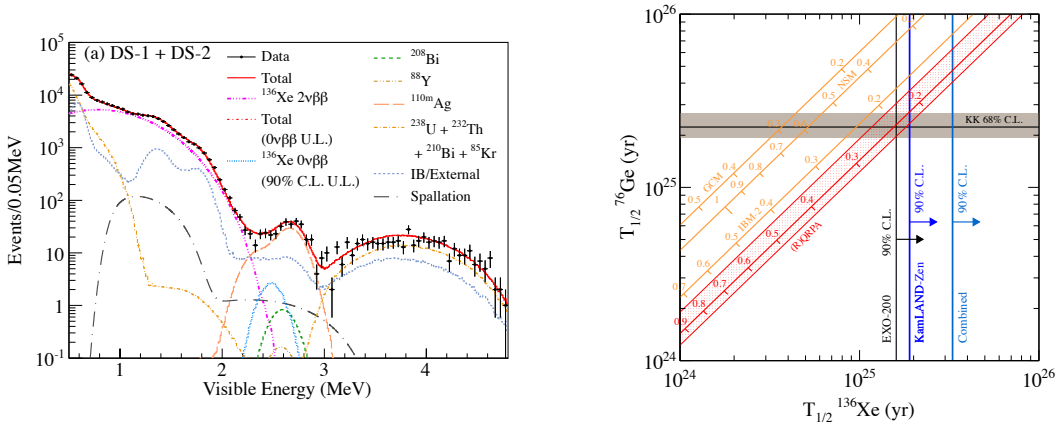

Figure 2: (Left) Visible energy spectrum of $\beta\beta$ candidates for DS1 and DS2, together with the best-fit spectral decomposition. (Right) Relationship between $T^{0\nu}_{1/2}$ of ^{76}Ge and ^{136}Xe as predicted by NME calculations (sloped lines), together with the limits on $T^{0\nu}_{1/2}$ of ^{136}Xe from EXO-200, KamLAND-Zen, and EXO+KamLAND combined (vertical lines). The claimed measurement in ^{76}Ge is shown by horizontal band.

Table 1: Summary of the parameters of the model and the constraints imposed in the likelihood fit.

	Parameter	Comments
Signal	$2\nu\beta\beta, 0\nu\beta\beta$	Both free
Backgrounds	^{222}Rn-^{210}Pb	Constrained by ^{214}Bi-^{214}Po study
	^{228}Th-^{208}Pb	Constrained by ^{212}Bi-^{212}Po study
	^{232}Th-^{228}Th (^{228}Ac)	Free
	^{238}U-^{222}Rn (^{234}Pa)	Free
	^{40}K, ^{85}Kr, ^{210}Bi	Free
	^{134}Cs,^{137}Cs	IB contribution constrained Xe-LS contribution free
	^{110m}Ag,^{60}Co,^{88}Y,^{208}Bi	Free
	^{10}C/^{10}C	Constrained by KamLAND spallation study
Detector response	A, k_B, R, σ	Constrained by calibration γ, tagged ^{214}Bi ($\beta+\gamma$) and neutron capture γ

measurement, for example calibration measurements for the detector response parameters or spallation studies for the spallation backgrounds. Where no constraint or measurement exists the parameter is allowed to vary freely in the fit.

2.5 Results

The best-fit rate of ^{136}Xe $2\nu\beta\beta$ decay is $82.9 \pm 1.1(\text{stat}) \pm 3.4(\text{syst})$ per (ton-day) for DS-1, and $80.2 \pm 1.8(\text{stat}) \pm 3.3(\text{syst})$ per ton-day for DS-2. These rates are consistent with EXO-200 [?] and an earlier halflife measurement, $T^{2\nu}_{1/2} = 2.30 \pm 0.02(\text{stat}) \pm 0.12(\text{syst})$, from KamLAND-Zen where the analysis was optimized for the $2\nu\beta\beta$ study [?]. The 90% C.L. upper limits on the number of ^{136}Xe $0\nu\beta\beta$ decays are < 16 and < 8.7 events for DS-1 and DS-2, respectively. Combining the results, we obtain a 90% C.L. lower limit of $T^{0\nu}_{1/2} > 1.9 \times 10^{25}$ yr. A simulation of an ensemble of experiments based on the best-fit background spectrum indicates a sensitivity of 1.0×10^{25} yr. The probability of obtaining a limit equal to or stronger than that just reported is 12%. A combination of the limits from KamLAND-Zen and EXO-200 yields the lower limit $T^{0\nu}_{1/2} > 3.4 \times 10^{25}$ yr (90% C.L.). The combined measurement has a sensitivity of 1.6×10^{25} yr, and the probability of obtaining a stronger limit is 7%. The corresponding 90% C.L. upper limit on $m_{\beta\beta}$ ranges between $m_{\beta\beta} < 120\,meV$ and $m_{\beta\beta} < 250\,meV$ depending on the NME

Table 2: Summary of exposure of ^{136}Xe

	DS1	DS2
livetime (days)	112.3	101.1
Fiducial Xe-LS mass (ton)	8.04	5.55
Xe loading (wt%)	2.44	2.48
^{136}Xe mass (kg)	179	125
^{136}Xe exposure (kg-yr)	54.9	34.6

Table 3: Summary of systematic uncertainties

Systematic Uncertainties	DS1	DS2
Fiducial Volume	3.9%	4.1%
Xe-concentration	0.34%	0.37%
Xe-enrichment	0.05%	0.05%
Energy scale	0.3%	0.3%
Detection Efficiency	0.2%	0.2%

calculations used [?]. The dominant source of systematic error in the $\beta\beta$ analysis comes from the fiducial volume estimate. The FV systematic error is estimated from the difference between the nominal fiducial volume and the fraction of ^{214}Bi events in the Xe-LS that pass the fiducial volume cuts. The systematic uncertainties on the $\beta\beta$ results are summarized in Table **??**.

The right side of Figure **??** compares these results with the detection claim in ^{76}Ge. The sloped lines indicate the relationship between $T^{0\nu}_{1/2}$ of ^{76}Ge and ^{136}Xe predicted by different NME calculations assuming $0\nu\beta\beta$ decay mediated by light Majorana neutrino exchange. The ^{76}Ge claim, as well as the lower limits on $T^{0\nu}_{1/2}$ of ^{136}Xe from EXO-200, KamLAND-Zen, and EXO-200 + KamLAND-Zen combined are shown. The combined limit for ^{136}Xe disagrees with the detection claim in ^{76}Ge at $> 97.5\%$ C.L. for all NME considered. This statement does not consider a statistical treatment of the NME uncertainties. An analysis attempting to treat the NME uncertainties statistically finds the disagreement is at 95.6% C.L significance [?].

3 Conclusion

The first phase of the KamLAND-Zen experiment was a very effective modification of the existing KamLAND detector which capitalized on the existing ultra-pure environment, detector, and data analysis infrastructure to quickly and efficiently realize a competitive $0\nu\beta\beta$ search. The combined KamLAND-Zen + EXO-200 limit provides the most stringent test to date on the ^{76}Ge claim. The KamLAND-Zen collaboration is currently working to reduce the background in the region of interest to improve the reach of the experiment.

Acknowledgments

The KamLAND/KamLAND-Zen experiments are supported by the Grant-in-Aid for Specially Promoted Research under Grant No. 21000001 of the Japanese Ministry of Education, Culture, Sports, Science and Technology; the World Premier Inter- national Research Center Initiative (WPI Initiative), MEXT, Japan; and under the US Department of Energy (DOE) Grant No. DE-AC02-05CH11231, as well as other DOE grants to individual institutions. The Kamioka Mining and Smelting Company has provided service for activities in the mine.

References

1. K. Zuber Journal of Physics G **39**, 12 (2012)
2. J. Beringer et *al.* (Particle Data Group) *Phys. Rev.* D **86**, 010001 (2012)
3. P. Vogel Journal of Physics G **39**, 12 (2012).
4. H. V. Klapdor-Kleingrothaus and I. V. Krivosheina *Mod. Phys. Lett.* A **21** 1547 (2006)
5. K. Eguchi et *al.* (KamLAND Collaboration) *Phys. Rev. Lett.* **90**, 021802 (2003).
6. S. Abe et *al.* (KamLAND Collaboration) *Phys. Rev.* C **81**, 025807 (2010)
7. A. Gando et *al.* (KamLAND-Zen Collaboration) *Phys. Rev.* C **86**, 021601 (R) (2010)
8. A. Gando et *al.* (KamLAND-Zen Collaboration) *Phys. Rev. Lett.* **110**, 062502 (2013)
9. M. Auger et *al.* (EXO Collaboration) *Phys. Rev. Lett.* **109**, 032505 (2012)